Applied Energy, Volume 242, 15 May 2019, pp. 1528-1538
DOI:10.1016/j.apenergy.2019.03.186

Simultaneous removal of SO_2 and NOx by a new combined spray-and-scattered-bubble technology based on preozonation: from lab scale to pilot scale

Tong Si[1], Chunbo Wang[1]*, Xuenan Yan[1], Yue Zhang[1], Yujie Ren[2], Jian Hu[2], Edward J. Anthony[3]

[1]Department of Energy Power & Mechanical Engineering, North China Electric Power University, Baoding 071003, China;

[2]CECEP Industrial Energy Conservation Co., Ltd, Beijing 100082, China

[3]School of Power Engineering, Cranfield University, Cranfield, Bedfordshire MK43 0AL, UK

*Corresponding author. Email address: hdwchb@126.com

Abstract: A new technology (called here, spray-and-scattered-bubble technology) based on preozonation was designed and tested for simultaneous removal of SO_2 and NOx from power plant flue gas. It combines the advantages of the common spray tower and the jet bubble reactor, in which the flue gas experiences an initial SO_2/NOx removal in the spray zone and then undergoes further removal in the bubble zone. Factors that affect the simultaneous removal of SO_2/NOx were investigated through lab-scale experiments, by varying the O_3/NO molar ratio, liquid/gas ratio and the immersion depth. The results showed the removal of SO_2 and NOx can be significantly improved as compared to a separate spray column or bubble reactor, by as much as 17%, for the spray column and 18% for the bubble reactor for NOx and 11% for the spray column, and 13% for the bubble reactor for SO_2, for liquid/gas ratio of 4 dm^3/m^3 or immersion depth of 100 mm. The O_3/NO molar ratio had little effect on the SO_2 removal, but it strongly affected the removal efficiency of NOx especially when it was less than 1.0. Both the liquid/gas ratio and immersion depth demonstrated a positive correlation with the removal efficiency. However, a balance must be maintained between efficiency and economics, since the liquid/gas ratio directly influences the performance and number of the circulating pumps, and the depth is closely related to the flue gas pressure drop, and both factors affect energy requirements. To further confirm its industrial feasibility, a 30 h test using real coal-fired flue gas was conducted in a pilot-scale experimental facility (flue gas volume of 5000 Nm^3/h). Increasing SO_2 concentration in flue gas can promote the removal efficiency of NOx, but the SO_2 removal was almost complete under all conditions tested. Finally, taking a 300 MW unit as an example, the total energy cost of this new technology is estimated as being 10% lower than that of the common spray tower technology, based on an analysis using Aspen Plus™, with the largest difference reflected in the energy requirements of the circulating pumps and the ozonizer. Over all, the new technology offers the joint advantages of reducing emissions and saving energy.

Keywords: Simultaneous SO_2 and NOx removal; Wet scrubber; Spray-and-scattered-bubble;

Energy consumption

1. Introduction

Coal-fired power generation accounts for more than 40% of global electricity supply and is expected to continue to play a key role in the energy sector [1]. However, due to the massive use of coal in power generation, coal-fired units are the main anthropogenic source of SO_2 and NOx [2]. In 2014, a new requirement for environmental protection called "ultra-low emission regulation (ULE)" was imposed by the Chinese government, in which the emission standards for SO_2 and NOx were limited to 35 mg/m^3 and 50 mg/m^3, respectively [3]. Wet flue gas desulfurization (WFGD) and selective catalytic reduction (SCR) are the most widely applied technologies for SO_2 and NOx control, respectively [4], [5]. To meet the increasingly stringent environmental requirements, a common method adopted is to increase the SCR catalyst layers (usually increased from 2 to 3 or 4 layers) for NOx abatement, and sometimes even adding another WFGD tower for SO_2. However, these methods always require additional energy input, which reduces the efficiency of the power plant [6], [7]. Therefore, simultaneous removal of SO_2 and NOx in a simplified system is a very attractive solution for this problem in the future.

The WFGD scrubber has the potential to be a multi-pollutant control device because of its excellent gas-liquid mass transfer [8]. However, due to the fact that NO accounts for almost 90% of the total NOx in coal-fired flue gas and only marginally dissolves in aqueous solution, the removal efficiency of NOx is normally extremely low [9]. Oxidizing NO to higher oxidation states (mainly NO_2 and N_2O_5) both of which have a higher solubility, can be used for the high-efficiency capture of NOx [10], [11]. It is known that O_3 is an effective oxidant for NO and avoids the need to introduce additional chemical additives such as $KMnO_4$ or $NaClO_2$ [12], [13]. In consequence, considerable research efforts have been devoted to reduce the power consumption of O_3 production. Sung et al. [14] developed a coaxial cylindrical-type dielectric barrier discharge ozonizer using a high-voltage pulse power system. The maximum production efficiency of the ozone generator can be as low as 12 kWh/kg. Malik et al. [15] studied the performance of a coupled surface discharge structure, the optimized power consumption for which is 16.7 kWh/kg. These clearly demonstrate that O_3 production tends to consume a large amount of energy, which becomes the dominant factor in reducing the commercial acceptance of this approach. To solve this problem, we propose a novel energy-saving wet scrubbing technology with preozonation.

According to the gas-liquid contacting pattern, scrubbing technology can be classified as either spray tower or jet bubble reactor (JBR). Given their simple structure, low resistance and low investment cost, spray towers have become the most commercially accepted wet scrubbers at present, especially in countries like China [16], [17]. Nonetheless, this technology has some issues. In particular, excess energy consumption is required to maintain operation of the circulating

pumps. In addition, problems with insufficient gas-liquid contact exist due to the relatively short residence time of flue gas in the tower. The JBR technology, developed by Chiyoda, abandons the circulating pumps and spray headers, making the system simpler than conventional spray towers [18]. Flue gas is jetted into a slurry, creating a foam layer on the liquid surface, which provides a very large interfacial area for reactions limited by mass transfer. However, the sparger tubes are usually immersed 200 mm or more below the liquid surface, causing ~2 kPa flue gas pressure drop [19]. This significant pressure drop severely restricts the industrial applications of JBR.

Designs of scrubbers that may enhance the removal capacity are shown in Table 1. These include the deflector spray tower, venturi scrubber, multi-stage tray scrubber, spray-cum-bubble scrubber and swirl cyclone scrubber. For most of the above approaches, the SO_2 removal efficiency was reported to be more than 98%. Adding internals or pre-treatment to control the flow pattern is also a common and effective method for increasing removal efficiency. However, the available internals also create energy efficiency problems. For example, the porous tray and venturi layers can result in a dramatic flue gas pressure loss and increased maintenance costs. Thus, the abovementioned technical routes to improve performance also introduce a greater energy burden if based on preozonation.

Table 1. Literature survey

Literatures	Scale	Scrubber types	Technical route for removal
Meikap et al. [20]	Laboratory	Venturi scrubber	Consist of cylindrical rods that can operate with lower liquid/gas ratio.
Chen et al. [21]	Laboratory	Deflector spray tower	Using deflectors, SO_2 removal efficiency can be improved while the pressure drop is decreased
Kurella et al [22]	Laboratory	Multi-stage plate wet scrubber	A three-stage dual-flow sieve plate column is used to increase the removal efficiency.
Zhong et al. [23]	Laboratory	Spray scrubber	A tangential coupling device is proposed to enhance the internal turbulence.
Mohan et al. [24]	Laboratory	spray-cum-bubble column scrubber	Experiments were conducted for spray section and bubble section separately, then combining both.
B&W company [25]	Industrial	dual-tray spray tower	A given amount of absorption liquid can be held within channels ranging from 25–40 mm, which offers additional gas-liquid contact.
BELCO company [26]	Industrial	EDV wet system	A patented nozzle is applied to form water film for improving sufficient contact.

To meet the need for a lower energy cost with strict adherence to environmental protection policy in the future, an entirely new techno-enviro-economic concept of scrubbing is proposed for simultaneous SO_2 and NOx removal, namely spray-and-scattered-bubble technology. As shown in Fig. 1, the new scrubber is divided into three parts: the demist zone; the spray zone; and the bubble zone. An aerosol eliminator and demister are located in the demist zone. One layer of spray headers containing nozzles is installed at the top of the spray zone. Sparger tubes are distributed

evenly at the bottom of the spray zone and immersed in the absorption slurry in the bubble zone. O_3 is first injected into the flue gas stream at the inlet of the spray zone. Mixed flue gas reacts with spray droplets in a co-current mode to achieve an initial SO_2/NOx removal in the spray zone, and further removal in the bubble zone. Gas free of SO_2/NOx is emitted into the atmosphere after demisting.

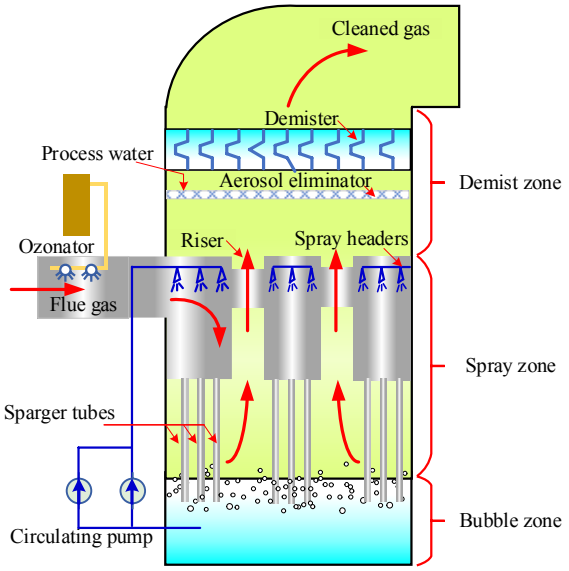

Fig. 1. The structure of the new spray-and-scattered-bubble tower

Fig. 2 shows the effects of liquid/gas ratio (L/G) and immersion depth on desulfurization efficiency in spray towers and JBR pipes [27], [28]. It can be seen from Fig. 2(a) that the desulfurization efficiency increases significantly in the range of 0~8 dm^3/m^3 L/G, indicating that the liquid/gas ratio has a staged effect on the SO_2 removal. Above 8 dm^3/m^3, only a marginal rise in efficiency is observed in the spray tower. Fig. 2(b) shows a similar tendency for desulfurization efficiency versus the immersion depth of JBR pipes. Hence, it seems that meeting much stricter environmental emission limits is only possible through increasing the liquid/gas ratio or the immersion depth, even though this requires an excessive energy expenditure. The present work marries the performance demonstrated in the two curves in Fig. 2 to achieve relatively lower energy consumption by reducing L/G and immersion depth. The removal efficiency of this concept is the same as or greater than that of the more energy-intensive traditional technology.

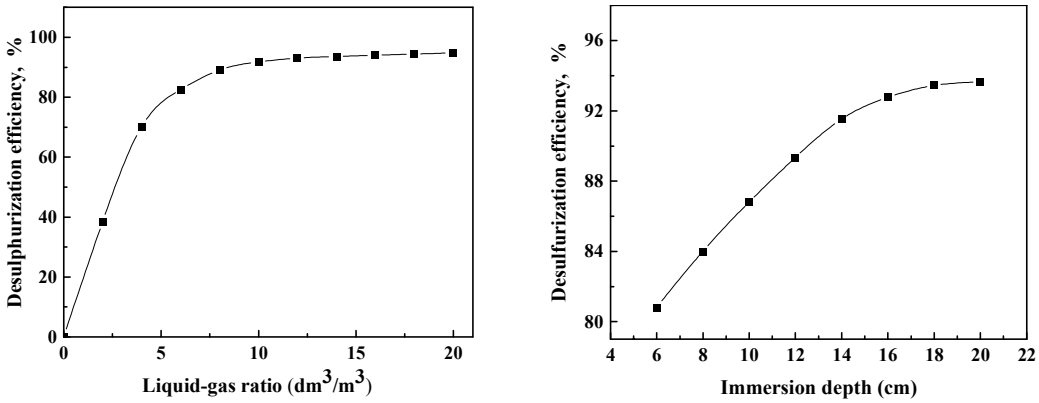

(a) Spray tower **(b) JBR**

Fig. 2. The desulfurization efficiency in the spray tower and jet bubbling reactor

The objective of this study is to investigate the simultaneous removal of SO_2 and NOx in a new spray-and-scattered-bubble tower. Some factors such as O_3/NO molar ratio, liquid/gas ratio, and immersion depth are evaluated to determine their effect. To further confirm its commercial application, 30 h of testing was carried out in a pilot-scale facility (flue gas volume of 5000 Nm^3/h) to verify the results from the lab-scale testing. Differences in energy consumption between the new technology and spray technology were compared using Aspen Plus™ software for a simple economic evaluation.

2. Experimental

2.1 Lab-scale apparatus

The experiments were conducted in a customized spray-and-scattered-bubble system, as shown in Fig. 3. The system is comprised of a wet scrubber, simulated flue gas generator and online flue gas analyzers.

The scrubber was made of synthetic glass, with a diameter of 450 mm and a height of 1.8 m. One layer of spray headers, which includes six spiral-type nozzles, was fixed at the top of the spray zone. Four PVC sparger tubes, each with a diameter of 30 mm, were distributed in circles above the liquid level. An electric stirrer was used to mix the holding tank at a pre-set speed to prevent slurry from precipitating. The inlet temperature was regulated by a temperature controller via electrical heating tubes and the pressure drop of the flue gas was monitored by a U-type manometer. Here, 99.9% SO_2 and 99.999% NO were supplied by compressed gas cylinders and O_3 originated from an oxygen source ozonizer (CF-G-3-5G, Guolin Co., China), the flow rates of which were controlled by flowmeters. Before the experimental process, the ozone concentration in the simulated flue gas was obtained by the iodometric method (according to the China National Standard CJ/T3028.2-94). Inlet and outlet concentrations of SO_2 (±1 mg/m^3), NO_2 (±1 mg/m^3), NO (±1 mg/m^3) were measured by two identical analyzers (Vario plus, MRU, Germany) after drying and all data were logged during testing.

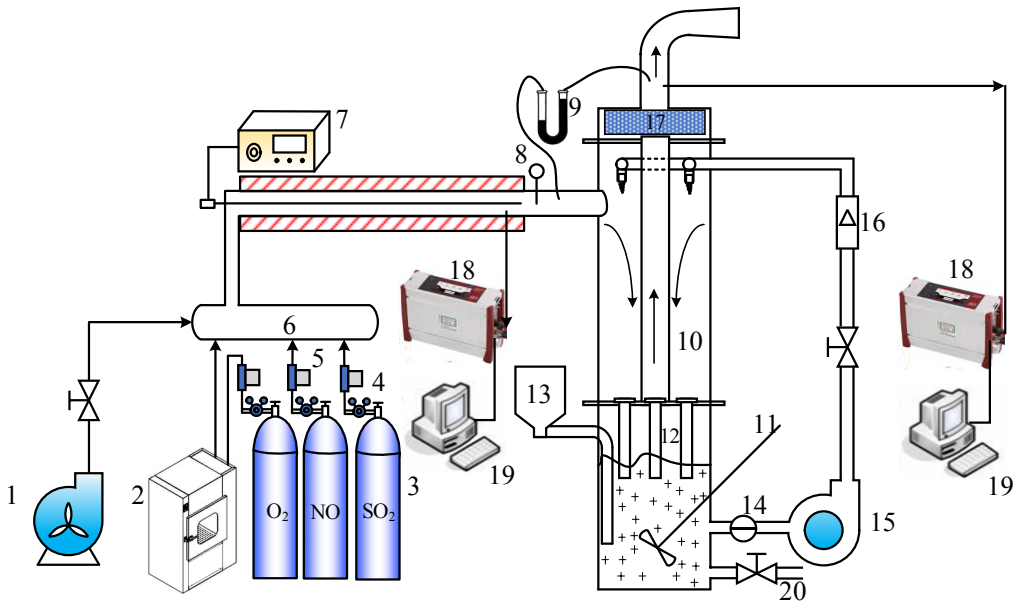

1-draught fan 2-ozone generator 3-gas cylinder 4-pressure reducing valve 5-flowmeter 6-mixer
7-temperature controller 8-thermometer 9-manometer 10-spray -and -bubble -scattered tower
11-electric stirrer 12 -sparger tubes 13 -slurry feeding tank 14-pH meter 15-circulating pump
16-flowmeter 17-demister 18-gas analyzers 19-computer 20 -discharge port

Fig. 3. Lab-scale spray-and-scattered-bubble experimental setup

2.2 Procedure

All measurements followed the same procedure. A known concentration of slurry (5 wt%) was loaded into the bubble zone to the desired immersion depth. The electric stirrer, heating tubes and circulating pump were then turned on and kept running continuously for at least 30 min to ensure the system achieved steady state. After that, simulated flue gas generation was started and the draught fan were switched on. Flowmeters were adjusted according to the display on the inlet gas analyzer and the outlet concentration was monitored at the same time.

Experimental condition details are listed in Table 2.

Table 2. Test parameters

Parameter	Value
Flue gas flow rate (m^3/h)	10
Inlet temperature (°C)	130
Inlet SO_2 concentration (mg/m^3)	2850-8550
Inlet NO concentration (mg/m^3)	230
Immersion depth (mm)	30-150
Liquid/gas ratio (dm^3/m^3)	2-18
Slurry pH	6.5

Because limestone could not be supplied continuously during testing, a pre-experiment was conducted to determine the appropriate duration of each test, thus guaranteeing data reliability.

The changes in removal efficiency and slurry pH with respect to time were evaluated, as shown in Fig. 4. (Conditions: liquid/gas ratio 8 dm^3/m^3, immersion depth 50 mm, SO_2 concentration 5500 mg/m^3)

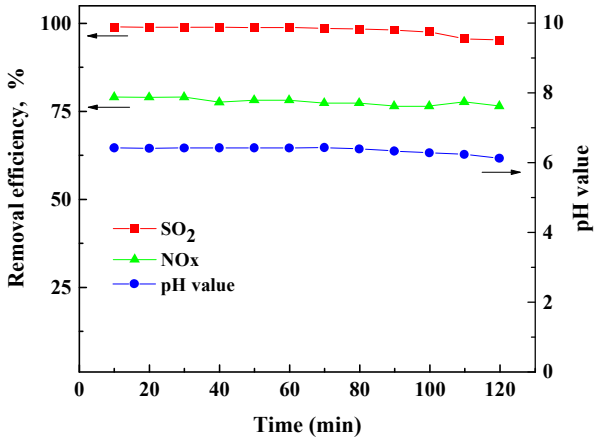

Fig. 4. The pre-experiment in the spray-and-scattered-bubble tower

Fig. 4 shows that both removal efficiency and slurry pH were almost independent of time within the first 100 min, indicating that quite stable conditions were achieved without the need to add additional limestone during the test. For example, the removal efficiency of SO_2 was always observed to be steady at about 99% after 100 min. As for the slurry pH, it tracked desulfurization efficiency, with the pH remaining at levels of about 6.2. The main reason for this is that the bubble zone can store enough slurry so that the effect of limestone consumption on removal efficiency can be neglected. Based on pre-testing, a duration of 60 min was selected to simulate continuous, stable operation.

2.3 Absorbent and data analysis

Baoding limestone was used for all testing. The main constituents are given in Table 3. Prior to the experiment, limestone was milled and sieved (0-0.044 mm).

Table 3. Baoding limestone analysis (wt%)

SiO_2	Al_2O_3	Fe_2O_3	TiO_2	P_2O_5	CaO	MgO	SO_3	Na_2O	K_2O	LOF
0.67	0.78	<0.10	<0.05	<0.03	54.93	<0.10	<0.10	<0.10	<0.10	42.90

The removal efficiency for SO_2 and NOx were calculated by using Eq. (1) and (2), respectively, where η is the removal efficiency; and C_{in} and C_{out} refer to the inlet and outlet pollutant concentration respectively, all concentration being expressed as mg/m^3.

$$\eta_{SO_2} = \frac{C_{SO_2,in} - C_{SO_2,out}}{C_{SO_2,in}} \times 100\% \quad (1)$$

$$\eta_{NOx} = \frac{C_{NOx,in} - C_{NOx,out}}{C_{NOx,in}} \times 100\% \quad (2)$$

3. Results and discussion

3.1 Lab-scale experiments

3.1.1 O_3/NO molar ratio

The effect of $n(O_3)/n(NO)$ on the removal efficiency was studied to obtain the optimal O_3 input value. Different $n(O_3)/n(NO)$ ratios were used by changing the flow rate of O_3. The SO_2 and NOx removal performances are shown in Fig. 5. (Conditions: SO_2 concentration 5500 mg/m^3, liquid/gas ratio 8 dm^3/m^3, immersion depth 50 mm.)

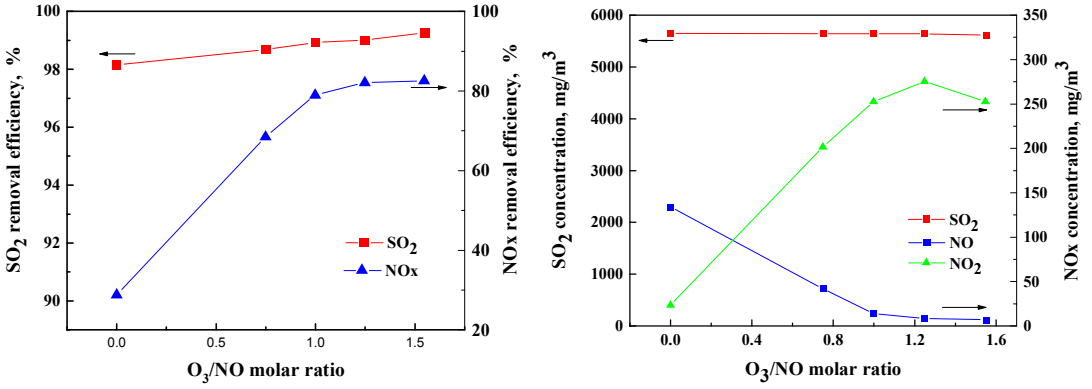

(a) (b)

Fig. 5. a-Effect of O_3 / NO ratio on SO_2 and NOx removal. b- Effect of O_3/NO ratio on SO_2 and NOx oxidation concentration.

As can be seen in Fig.5(a), with the increase of $n(O_3)/n(NO)$, the removal efficiency of NOx increases rapidly and then tends to level off. For example, when $n(O_3)/n(NO)$ is increased from 0 to 1.0, the removal efficiency of NOx increases linearly from 28.7% to 79.8%. After that as $n(O_3)/n(NO)$ further increases to 1.5, the removal efficiency of NOx increases by only 3%, while the removal efficiency of SO_2 remains almost constant throughout the experiment. It can be concluded that the $n(O_3)/n(NO)$ has little impact on the removal efficiency of SO_2.

To understand the absorption behavior of SO_2 and NOx in more detail, the oxidation concentrations of the main oxides were studied separately, as shown in Fig. 5(b). It is clear that the SO_2 concentration is almost independent of the $n(O_3)/n(NO)$, as can be seen from the small variation in removal efficiency of SO_2 (Fig. 5(a)). However, the curves for nitrogen oxides concentrations show different tendencies and they can be divided into two stages: (i) When $n(O_3)/n(NO)$ varies from 0 to 1.0, NO concentration drops sharply to almost zero and NO_2 concentration increases accordingly, indicating that NO_2 is the dominant product as described in Eq. (3)-(5) [29]. As expected, the removal efficiency of NOx significantly increases because of its much higher solubility in the form of NO_2, as can be seen in Fig. 5(a). (ii) When $n(O_3)/n(NO)$ reaches a value of 1.5, NO_2 concentration decreases by almost 30 mg/m^3 compared with the maximum value (about 287 mg/m^3). This is mainly because, by this time excess O_3 causes NO_2 to

be oxidized to N_2O_5 according to Eq. (6)-(7). The reaction between N_2O_5 and water, as shown by Eq. (8) is fast, resulting in a stable removal efficiency for NOx [30].

$$NO + O_3 \rightarrow NO_2 + O_2 \tag{3}$$

$$O_3 + N \rightarrow O_2 + NO \tag{4}$$

$$NO + O(+M) \rightarrow NO_2(+M) \tag{5}$$

$$NO_2 + O_3 \rightarrow NO_3 + O_2 \tag{6}$$

$$NO_3 + NO_2 \rightarrow N_2O_5 \tag{7}$$

$$N_2O_5 + H_2O \rightarrow 2HNO_3 \tag{8}$$

It can be concluded that SO_2 and NOx can be removed efficiently by the new technology. When $n(O_3)/n(NO)$ approaches 1.0, the removal efficiency reaches the emission limit. The following work was conducted based on this condition.

3.1.2 Liquid/gas ratio

By changing the flow rate of the cycled slurry, a series of runs was performed to investigate the effect of liquid/gas ratio on the simultaneous removal of SO_2 and NOx, as shown in Fig. 6. Meanwhile, two removal modes (spray only and the new technology presented here) were chosen for comparison. The sparger tubes were placed 100 mm above the liquid level during the spray-only process, which guarantees the flue gas can directly be exhausted to the atmosphere without passing through the bubble zone. Meanwhile, considering the possible reaction between the flue gas and the liquid surface of the bubble zone, the SO_2 absorption experiment without spraying was carried out as a baseline. During spray-only operation, effects which may result from the liquid surface absorption will be eliminated. (Conditions: SO_2 concentration 5500 mg/m^3, immersion depth 50 mm)

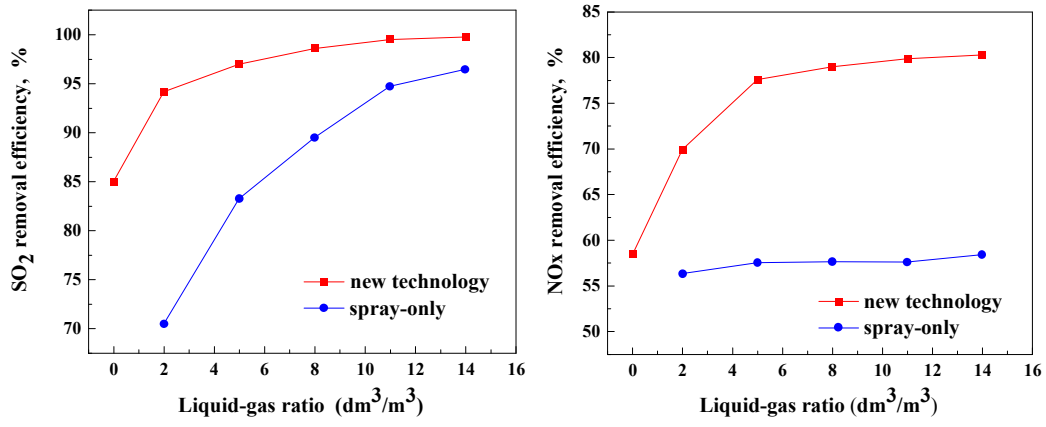

(a) SO_2 (b) NOx

Fig. 6. Effect of liquid/gas ratio on SO_2 and NOx removal

It can be seen in Fig. 6 that this new technology significantly improves the removal efficiency of SO_2 and NOx compared with spray-only for the current testing conditions. Although the removal efficiency of SO_2 with a given liquid-gas ratio shows a very similar behavior for different technologies, the removal efficiency for NOx is significantly different.

In Fig. 6(a), for both modes, the desulfurization efficiency increases rapidly with liquid/gas ratio and then stabilizes gradually. The main reason for this is that there is a larger contact area between SO_2 and the spray droplets in the spray zone when the liquid/gas ratio increases, leading to enhanced absorption capacity. When the liquid/gas ratio is 2 dm^3/m^3, the removal efficiency of SO_2 quickly reaches 94.1% and after that changes little, whereas it continues to increase rapidly in the experimental range for spray-only. Considering that the liquid/gas ratio is the most crucial index for evaluating the performance and economy of a desulfurization technology, this means that the SO_2 reaction rate has been greatly enhanced by this combined technology.

In Fig. 6(b), it can be seen that the removal efficiency of NOx has a similar behavior to SO_2 in the new technology, but there is a significant difference with the spray-only results, which indicates that the bubbling reaction clearly improves the removal efficiency of NOx. This phenomenon may be attributable to the fact that the sulfite ion can be produced in the spray zone and enriched in the bubble zone, and can significantly accelerate the denitration rate according to Eq. (9)-(10) [31], [32]. However, according to the results of Ma et al. [30], the increase of liquid/gas ratio decreases the sulfite concentration on the droplet surface, which weakens the reaction between NO_2 and sulfite to some extent, thereby decreasing the removal efficiency of NOx. Hence, the removal efficiency of NOx levels off above a certain liquid/gas ratio.

$$2NO_2 + SO_3^{2-} + H_2O \rightarrow 2NO_2^{-} + SO_4^{2-} + 2H^+ \quad (9)$$

$$2NO_2 + HSO_3^{-} + H_2O \rightarrow 2NO_2^{-} + SO_4^{2-} + 3H^+ \quad (10)$$

3.1.3 Immersion depth

Immersion depth refers here to the vertical distance between the bottom of the sparger tubes and the stationary level of the slurry. By adjusting the level of the slurry, the effects of immersion depth were elucidated, as shown in Fig. 7. Because only a slight increase in removal efficiency is observed when the liquid/gas ratio exceeds 6 dm^3/m^3, this ratio was chosen for the testing. (Conditions:SO_2 concentration 5500 mg/m^3.)

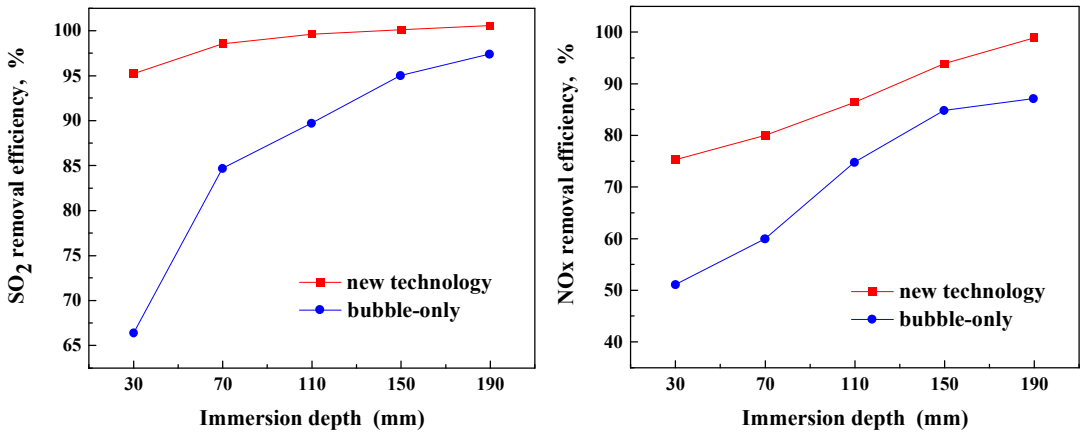

(a) SO_2 (b) NOx

Fig. 7. Effect of immersion depth on SO_2 and NOx removal

It can be seen from Fig.7(a) that the immersion depth has only a small effect on the removal of SO_2 in the new technology compared with the JBR. For example, the removal efficiency of SO_2 in the JBR technology increases approximately linearly from 66.7% to 94.5% when immersion depth rises from 30 to 150 mm, but for the new technology, only a minor increase from 95.2% to 99.6% is observed. The main reason for this is that most of the SO_2 can be removed in the spray zone and, therefore, the bubble zone has enough absorption capacity for the remaining SO_2, even with an immersion depth of 30 mm. Also, the increased immersion depth does little for the further capture of SO_2.

In Fig. 7(b), the combined technology can always achieve better capture of NOx than that of the JBR technology, and higher NOx removal efficiency corresponds to a greater immersion depth for both technologies. This is because the removal of NOx is mainly carried out in the bubble zone. At the same time, the reaction between NOx and water is much faster than SO_2 and water, so that the removal efficiency of NOx is more sensitive than SO_2 to immersion depth [30].

Additionally, as indicated by Fig. 7 with the increase of immersion depth, eventually the removal efficiencies of SO_2 and NOx using the JBR will approach those in this new technology. However, since the depth is related to the pressure drop of flue gases, process economics need to be considered when choosing the best immersion depth.

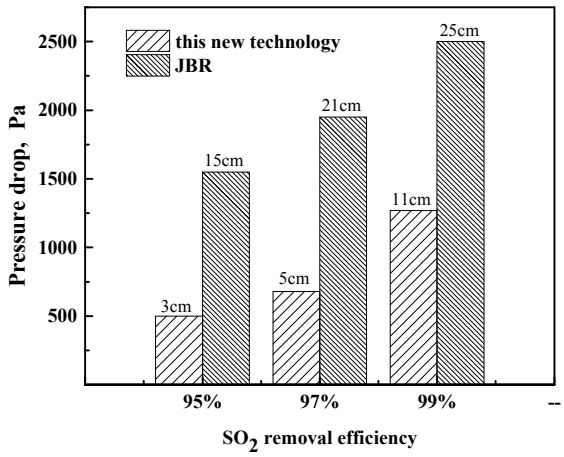

Fig. 8. Effect of immersion depth on pressure drop

Fig. 8 shows the pressure drop of the two modes at different desulfurization efficiencies. The pressure drop can be decreased by this new technology under the same efficiency conditions. For example, the pressure drop of the JBR is twice as high as that of this new technology when the desulfurization efficiency reaches 99%, which represents the current emission targets for the majority of power plants. This means that the economic operating benefits of this new technology are exceptional as compared to the conventional JBR technology. Thus, the selection of a suitable immersion depth is essential to the functioning of an effective spray-and-scattered-bubble tower.

3.2 Pilot-scale testing

To validate the industrial applicability of the lab-scale results, a pilot-scale spray-and-scattered-bubble tower was established in Shanxi province, China, and the testing was carried out with actual coal-fired flue gas. To maintain the liquid-level and pH within the required range, fresh slurry and process water were added continuously during the pilot-scale tests.

3.2.1 Pilot-scale apparatus

The pilot-scale apparatus and distributed control system (DCS) operation interface are shown in Fig. 9. The flue gas was from a 440 t/h pulverized coal boiler. A maximum flow of 5000 Nm^3/h was introduced to the pilot-scale setup through a bypass pipeline from the exit of the economizer. A pilot-scale spray-and-scattered-bubble tower (1.3 m in external diameter and 7.5 m in height, constructed of 316L stainless steel) was used for testing. The flue gas passed through a hot-gas filter to reduce the dust concentration to about 10 mg/m^3 before it entered the tower. At the same time, its temperature was decreased to less than 150 °C by a heat exchanger. A liquid oxygen tank supplied high-purity oxygen to an ozonizer (CF-G-2-5kg, Guolin Co, China).

(a) Pilot-scale apparatus

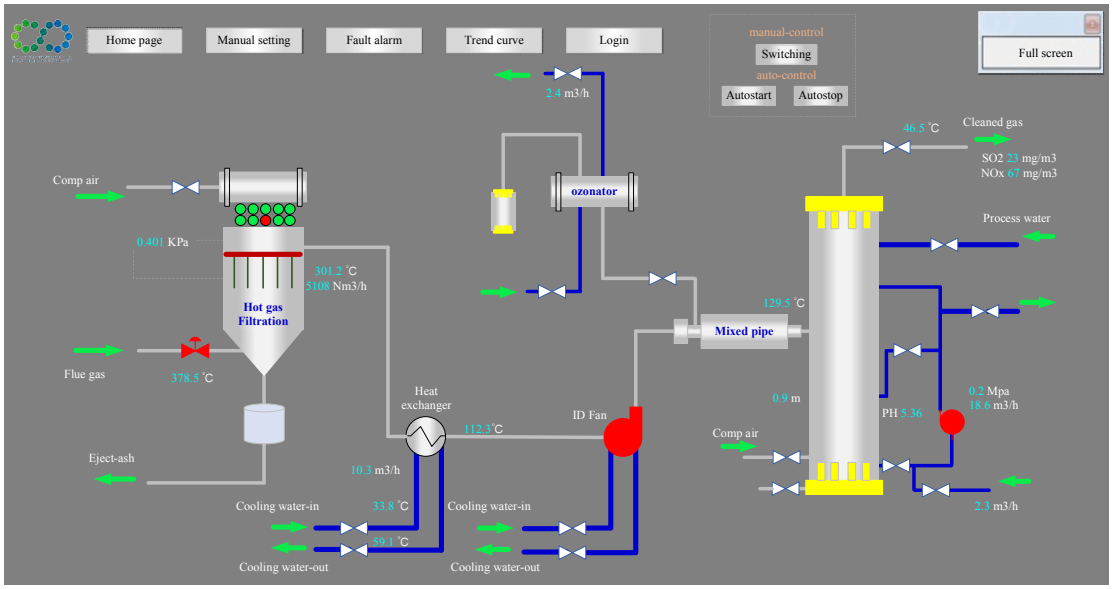

(b) DCS operation interface

Fig. 9. Pilot-scale experimental setup

3.2.2 30 hour test run

Similar to the lab-scale experiments, the three removal modes were tested over 30 h of operation, with the aim of further confirming the industrial feasibility of this new technology. (Conditions: liquid/gas ratio 4 dm^3/m^3, immersion depth 100 mm, SO_2 concentration ~2200mg/m^3)

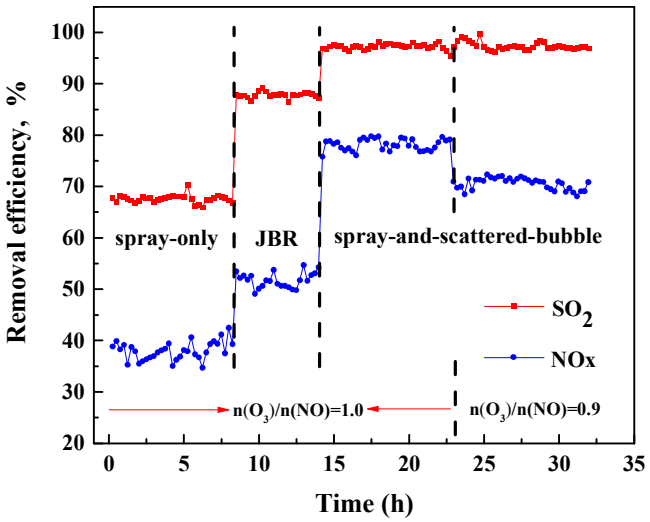

Fig. 10. 30 h operation in 5000 Nm^3/h pilot-scale experimental setup

As shown in Fig.10, neither the spray technology nor the JBR were able to meet the ultra-low emission limits [33]. This is mainly due to the lower liquid/gas ratio and shallower immersion depth. Usually the spray technology has higher desulfurization efficiency than the bubble technology, but it is interesting that during this testing, the spray technology achieved only ~70% removal efficiency in desulfurization, which is far less than that of the bubble technology. A probable explanation for this is that the pattern of gas-liquid contact for this particular spray unit is co-current, reducing the degree of reaction and, thus the removal efficiency.

In addition, it can be seen in Fig. 10 that for both the desulfurization and denitration, this new technology has the highest removal efficiency among the three technologies, which demonstrates that this process is industrially attractive. Taking $n(O_3)/n(NO)=1.0$ for example, the removal of SO_2 and NOx can be improved compared with the spray tower or JBR technology, increasing by about 28% for the spray tower, and 37% for the JBR for NOx and 11%, for the spray tower and 25%, for the JBR for SO_2 under the same conditions. These results demonstrate the synergic effect of combining these two technologies and the potential benefits available from this new system. Moreover, the removal efficiency of SO_2 is not significantly affected by the change of $n(O_3)/n(NO)$, mainly due to the fact that its reaction activation energy with O_3 is higher than for NOx. Also, the removal efficiency of NOx decreases with the reduction of $n(O_3)/n(NO)$, which is the same results seen from the lab work discussed in section 3.1.1.

3.2.3 Effect of SO_2 concentration

The SO_2 concentration in flue gas is determined by the sulfur content of the coal, and understanding the effect of SO_2 concentration on removal performance is of great significance for evaluating the units. Thus, three concentrations of SO_2 (~2200, 3400 and 4500 mg/m^3) were produced by burning different types of coal. The inlet NOx concentration remained essentially the same (460~480 mg/m^3) by making minor combustion adjustments, as shown in Fig. 11.

(Conditions: n(O_3)/n(NO) 1.0, liquid/gas ratio 4 dm^3/m^3, immersion depth 100 mm.)

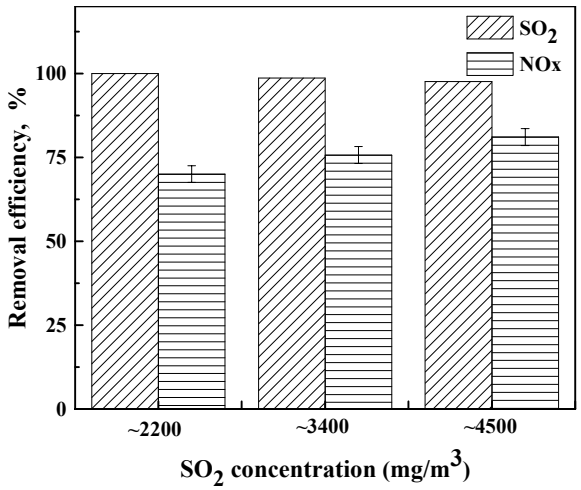

Fig. 11. Effect of SO_2 concentration on SO_2 and NOx removal

It can be seen from Fig.11 that higher SO_2 is helpful for improving the removal efficiency of NOx. For instance, the removal efficiency of NOx is increased by more than 10% when SO_2 concentration rises from 2200 to 4500 mg/m^3. A similar phenomenon was observed by Chandrasekara et al. [34], who also studied the removal performance of NOx by changing the feed concentration of SO_2. However, Fig. 11 also shows that the impact of SO_2 concentration on its own removal is not as significant as it is on NOx. It can be concluded that the SO_2 concentration over the ranges studied has little impact on removal efficiency of SO_2, indicating that a broad range of fuels could be used with this new technology. The reason for this phenomenon may be that SO_2 in the flue gas undergoes removal in two stages, which results in a significant reduction in the SO_2 partial pressure [35]. The dynamic equilibrium is maintained between the absorption rate and driving force, so that the desulfurization efficiency is almost unaffected by SO_2 concentration.

4 Energy consumption

The WFGD system is not only an environmental protection device, but also an energy consumption system. Usually, it will consume approximately 1%-3% of the total power generation, the main sources including circulating pumps, the booster fan and the ozonizer. Here, taking a 300 MW unit as an example, the energy consumption during the operation between spray technology and this new technology is analyzed with Aspen Plus V8.6 software.

4.1 System flowsheet and parameter introduction

To simplify the simulation process, the following assumptions are made:

(1) components such as CO_2 in the flue gas are not involved in the reaction and the influence of dust is not considered; (2) solids are not considered; and (3) the desulfurization system is assumed to operate under stable conditions.

Here, two Ca-based SO_2 absorption systems are assigned as shown in Fig. 12. and the differences are represented in the dashed box. Specifically in this new technology, the cocurrent contact of gas-liquid in spray zone is similar to the single-stage contact operation, hence an equivalent cocurrent model is established. During this process, the inlet temperature of the flue gas is 130 °C, and the total flow rate is 1.2×10^6 m^3/h. The volume fraction of flue gas components is shown in Table 4. Mass fraction of the limestone slurry is 25% and the operation temperature is about 50 °C.

Table 4. Gas components of flue gas

Parameters	$\varphi(N_2)$/%	$\varphi(CO_2)$/%	$\varphi(O_2)$/%	$\varphi(H_2O)$/%	$\varphi(SO_2)$/%	φ(NO)/%
Value	73.6	13.18	5.7	7.4	0.095	0.025

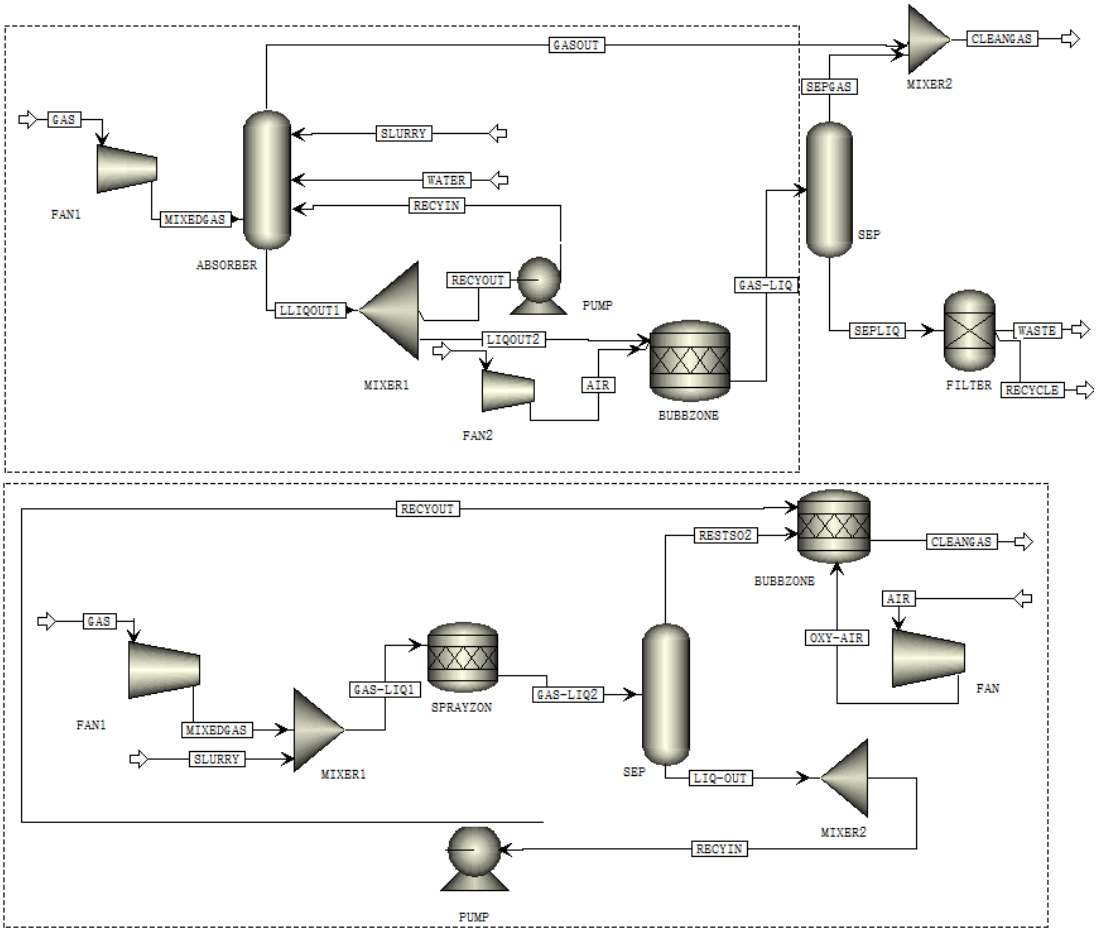

Fig.12 Flowsheets for the Aspen Plus model

4.2 Selection of model

Due to the electrolyte components involved in the reaction system, the property method of the whole process simulation uses the electrolyte-NRTL model in Aspen Plus. After that, two element cross correlation parameters and electrolyte equivalent parameters are called from the database automatically. Reactions are maintained at equilibrium state and polytropic compression

using the ASME method is applied to the pressure changers.

4.3 Simulation results

The simulation results are shown in Table. 4 and for clarity of discussion, the energy consumption is also presented in Fig. 13. The total energy consumption of this new technology is approximately 10% lower than that of the spray technology. At the same time, the largest differences are reflected in the circulating pump and the ozonizer. In the new technology, the consumption proportion of the circulating pump accounts for less than 10% of the total, which is far less than that of the spray technology. This occurs because the dramatic decrease of liquid/gas ratio and spray layers in the new technology, results in a decrease in the number of circulating pumps. It should be noted that more than 50% of the energy consumption is attributed to the ozonizer in this new technology; and this is where further improvement is needed in the future. The new technology clearly demonstrates the joint advantages of saving energy and reducing emissions.

Table 4. Simulation results

	Circulating pump		Booster fan		Ozonizer
	spray technology	new technology	spray technology	new technology	new technology
Fluid/Indicated power (kW)	1566.07	417.62	971.3	1621.69	——
Brake power (kW)	1740.08	464.02	1022.43	1707.04	——
Electricity (kW)	1933.42*3	515.58	1022.43	1707.04	3857.14
Pressure change (MPa)	0.2	0.2	0.004	0.005	——
Head developed (m)	26.62	26.62	——	——	——
Efficiency used	0.9	0.9	0.95	0.95	——
Outlet temperature (°C)	55.37	56.28	113	115	25
Outlet pressure (MPa)	0.3	0.3	0.1	0.1	0.098

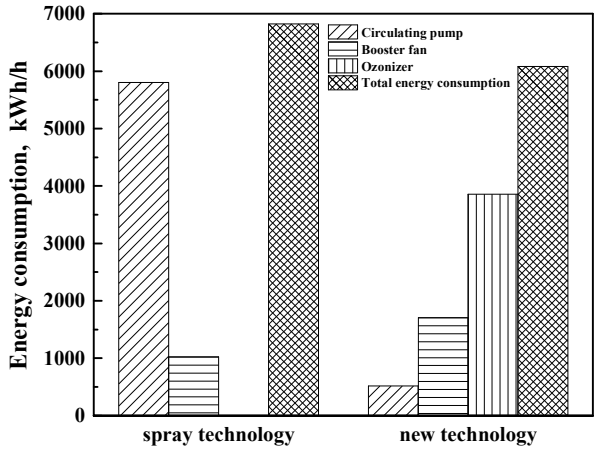

Fig. 13. Energy consumption: spray technology vs. new technology

5 Conclusions

This work focuses on the simultaneous removal of SO_2 and NOx by a new scrubbing technology, including lab testing and pilot-scale application. The energy consumption and the effect of different process parameters were explored.

(1) From the lab testing: the desulfurization and denitration processes can be improved by the new combined spray-and-scattered-bubble technology based on preozonation compared with spray or jet bubble reactor technology, with removal efficiency increased by as much as 17%, for the spray column and 18% for the bubble reactor for NOx and 11% for the spray column, and 13% for the bubble reactor for SO_2, for liquid/gas ratio of 4 dm^3/m^3 or immersion depth of 100 mm. The O_3/NO molar ratio has a marginal effect on the removal efficiency of SO_2, but it greatly affects the removal efficiency of NOx, especially when the value is less than 1.0. Both the liquid/gas ratio and the immersion depth had a positive correlation with the removal efficiency, but the power consumption of the circulating pumps and the pressure drop of flue gases must be taken into consideration.

(2) From the pilot-scale application: this new technology demonstrates the highest removal efficiency among the three modes using real coal-fired flue gas during 30 h operation. With increasing SO_2 concentration, SO_2 was characterized as a promotor of NOx removal, but the desulfurization efficiency was almost constant in all tests, indicating a strong adaptability for various coal types.

(3) The energy consumption of the main equipment in this new technology is 10% lower than that of the traditional spray technology. This is attributed to the dramatic decrease of liquid/gas ratio and spray layers even though the ozonizer consumes relatively large quantities of energy.

6 Acknowledgement

The financial support from the National Key R&D Program of China (No.2016YFB0600701) and Fundamental Research Funds for the Central Universities (2018ZD03, 2018QN083) are gratefully acknowledged.

References:

1. Wang C, Liu H, Zhang Y, Zou C, Anthony EJ. Review of arsenic behavior during coal combustion: Volatilization, transformation, emission and removal technologies. Progress in Energy and Combustion Science 2018;68:1-28. http://doi.org/10.1016/j.pecs.2018.04.001.

2. Li K, Yu H, Qi G, Feron P, Tade M, Yu J, Wang S. Rate-based modelling of combined SO_2 removal and NH_3 recycling integrated with an aqueous NH_3-based CO_2 capture process. Applied Energy 2015;148:66-77. http://doi.org/10.1016/j.apenergy.2015.03.060.

3. Hao R, Yang S, Yuan B, Zhao Y. Simultaneous desulfurization and denitrification through an integrative process utilizing $NaClO_2/Na_2S_2O_8$. Fuel Processing Technology 2017;159:145-152. http://doi.org/10.1016/j.fuproc.2017.01.018.

4. Gao X, Ding H, Du Z, Wu Z, Fang M, Luo Z, Cen K. Gas–liquid absorption reaction between $(NH_4)_2SO_3$ solution and SO_2 for ammonia-based wet flue gas desulfurization. Applied Energy 2010;87:2647-2651. http://doi.org/10.1016/j.apenergy.2010.03.023.

5. Liang Z, Ma X, Lin H, Tang Y. The energy consumption and environmental impacts of SCR technology in China. Applied Energy 2011;88:1120-1129. http://doi.org/10.1016/j.apenergy.2010.10.010.

6. Zhang L, Wang D, Liu Y, Kamasamudram K, Li J, Epling W. SO_2 poisoning impact on the NH_3-SCR reaction over a commercial Cu-SAPO-34 SCR catalyst. Applied Catalysis B: Environmental 2014;156-157:371-377. http://doi.org/10.1016/j.apcatb.2014.03.030.

7. Liu Y, Liu Z, Wang Y, Yin Y, Pan J, Zhang J, Wang Q. Simultaneous absorption of SO_2 and NO from flue gas using ultrasound/Fe^{2+}/heat coactivated persulfate system. Journal of Hazardous Materials 2018;342:326-334. http://doi.org/10.1016/j.jhazmat.2017.08.042.

8. Hutson ND, Krzyzynska R, Srivastava RK. Simultaneous Removal of SO_2, NOx, and Hg from Coal Flue Gas Using a $NaClO_2$-Enhanced Wet Scrubber. Industrial & Engineering Chemistry Research 2008;47:5825-5831. http://doi.org/10.1021/ie800339p.

9. Zheng C, Xu C, Zhang Y, Zhang J, Gao X, Luo Z, Cen K. Nitrogen oxide absorption and nitrite/nitrate formation in limestone slurry for WFGD system. Applied Energy 2014;129:187-194. http://doi.org/10.1016/j.apenergy.2014.05.006.

10. Zhao Y, Hao R, Guo Q, Feng Y. Simultaneous removal of SO_2 and NO by a vaporized enhanced-Fenton reagent. Fuel Processing Technology 2015;137:8-15. http://doi.org/10.1016/j.fuproc.2015.04.003.

11. Liu Y, Wang Q, Pan J. Novel process on simultaneous removal of nitric oxide and sulfur dioxide using vacuum ultraviolet (VUV)-activated $O_2/H_2O/H_2O_2$ system in a wet VUV-spraying reactor. Environmental Science & Technology 2016;50:12966-12975.

12. Yoon HJ, Park H, Park D. Simultaneous oxidation and absorption of NOx and SO_2 in an integrated O_3 oxidation/wet atomizing system. Energy & Fuels 2016;30:3289-3297. http://doi.org/10.1021/acs.energyfuels.5b02924.

13. Zhou S, Zhou J, Feng Y, Zhu Y. Marine emission pollution abatement using ozone oxidation by a wet scrubbing method. Industrial & Engineering Chemistry Research 2016;55:5825-5831. http://doi.org/10.1021/acs.iecr.6b01038.

14. Sung TL, Teii S, Liu CM, Hsiao RC, Chen PC, Wu YH, Yang CK, Teii K, Ono S, Ebihara K. Effect of pulse power characteristics and gas flow rate on ozone production in a cylindrical dielectric barrier discharge ozonizer. Vacuum 2013;90:65-69. http://doi.org/10.1016/j.vacuum.2012.10.003.

15. Malik MA, Schoenbach KH, Heller R. Coupled surface dielectric barrier discharge reactor-ozone synthesis and nitric oxide conversion from air. Chemical Engineering Journal 2014;256:222-229. http://doi.org/10.1016/j.cej.2014.07.003.

16. Wu XM, Qin Z, Yu YS, Zhang ZX. Experimental and numerical study on CO_2 absorption mass transfer enhancement for a diameter-varying spray tower. Applied Energy 2018;225:367-379. http://doi.org/10.1016/j.apenergy.2018.04.053.

17. Codolo MC, Bizzo WA. Experimental study of the SO_2 removal efficiency and volumetric mass transfer coefficients in a pilot-scale multi-nozzle spray tower. International Journal of Heat and Mass Transfer 2013;66:80-89. http://doi.org/10.1016/j.ijheatmasstransfer.2013.07.011.

18. Zheng Y, Kiil S, Johnsson JE. Experimental investigation of a pilot-scale jet bubbling reactor for wet flue gas desulphurisation. Chemical Engineering Science 2003;58:4695-4703. http://

doi.org/10.1016/j.ces.2003.07.002.
19. Zhou G, Zhong W, Zhou Y, Wang J, Wang T. 3D simulation of sintering flue gas desulfurization and denitration in a bubbling gas absorbing tower. Powder Technology 2017;314:412-426. http://doi.org/10.1016/j.powtec.2016.09.051.
20. Bal M, Reddy TT, Meikap BC. Performance evaluation of venturi scrubber for the removal of iodine in filtered containment venting system. Chemical Engineering Research and Design 2018;138:158-167. http://doi.org/10.1016/j.cherd.2018.08.019.
21. Chen Z, Wang H, Zhuo J, You C. Experimental and numerical study on effects of deflectors on flow field distribution and desulfurization efficiency in spray towers. Fuel Processing Technology 2017;162:1-12. http://doi.org/10.1016/j.fuproc.2017.03.024.
22. Kurella S, Meikap BC. Removal of fly-ash and dust particulate matters from syngas produced by gasification of coal by using a multi-stage dual-flow sieve plate wet scrubber. Journal of Environmental Science and Health, Part A 2016;51:870-876. http://doi.org/10.1080/10934529.2016.1181465.
23. Zhong Y, Gao X, Huo W, Luo Z, Ni M, Cen K. A model for performance optimization of wet flue gas desulfurization systems of power plants. Fuel Processing Technology 2008;89:1025-1032. http://doi.org/10.1016/j.fuproc.2008.04.004.
24. Raj Mohan B, Meikap BC. Performance characteristics of the particulate removal in a novel spray-cum-bubble column scrubber. Chemical Engineering Research and Design 2009;87:109-118. http://doi.org/10.1016/j.cherd.2008.05.011.
25. Guo BY, Hou QF, Yu AB, Li LF, Guo J. Numerical modelling of the gas flow through perforated plates. Chemical Engineering Research and Design 2013;91:403-408. http://doi.org/10.1016/j.cherd.2012.10.004.
26. Li H. Study of FCC Regenerated flue gas pollutant purification scheme (in Chinese). Shanghai: East China University of Science and Technology; 2013.
27. Chen Z, Wang H, Zhuo J, You C. Enhancement of mass transfer between flue gas and sl urry in the wet flue gas desulfurization spray tower. Energy & Fuels 2018;32:703-712. http://doi.org/10.1021/acs.energyfuels.7b03009.
28. Bai Y., Li Y., Cen K. Simultaneous absorption of SO_2 and NO from flue gas with $KMnO_4/CaCO_3$ slurry (in Chinese). Journal of China Coal Society 2008;33:575-578.
29. Zhou S, Zhou J, Feng Y, Zhu Y. Marine emission pollution abatement using ozone oxidation by a wet scrubbing method. Industrial & Engineering Chemistry Research 2016;55:5825-5831. http://doi.org/10.1021/acs.iecr.6b01038.
30. Ma Q, Wang Z, Lin F, Kuang M, Whiddon R, He Y, Liu J. Characteristics of O_3 oxidat ion for simultaneous desulfurization and denitration with limestone-gypsum wet scrubbing: appli cation in a carbon black drying kiln furnace. Energy & Fuels 2015;30:2302-2308. http://doi.org/10.1021/acs.energyfuels.5b02717.
31. Tang N, Liu Y, Wang H, Xiao L, Wu Z. Enhanced absorption process of NO_2 in $CaSO_3$ slurry by the addition of $MgSO_4$. Chemical Engineering Journal 2010;160:145-149. http://doi.org/10.1016/j.cej.2010.03.022.
32. Littlejohn D, Wang Y, Chang S. Oxidation of Aqueous Sulfite Ion by Nitrogen Dioxide. Environmental Science and Technology 1993;27:2162-2167.
33. Cui S, Hao R, Fu D. An integrated system of dielectric barrier discharge combined with wet electrostatic precipitator for simultaneous removal of NO and SO_2: Key factors assessments, products analysis and mechanism. Fuel 2018;221:12-20. http://doi.org/10.1016/j.fuel.2018.02.078.

34. Chandrasekara Pillai K, Chung SJ, Raju T, Moon I. Experimental aspects of combined NOx and SO_2 removal from flue-gas mixture in an integrated wet scrubber-electrochemical cell system. Chemosphere 2009;76:657-664. http://doi.org/10.1016/j.chemosphere.2009.04.013.
35. Rahmani F, Mowla D, Karimi G, Golkhar A, Rahmatmand B. SO_2 removal from simulate d flue gas using various aqueous solutions: absorption equilibria and operational data in a pack ed column. Separation and Purification Technology 2015;153:162-169. http://doi.org/10.1016/j.sep pur.2014.10.028.